Materials Letters 172 (2016) 81–84

Contents lists available at ScienceDirect

Materials Letters

journal homepage: www.elsevier.com/locate/matlet

3D interconnected porous carbons from MOF-5 for supercapacitors

Moxin Yu [a], Li Zhang [a], Xiaojun He [a,*], Huanhuan Yu [a], Jiufeng Han [a], Mingbo Wu [b,*]

[a] School of Chemistry and Chemical Engineering, Anhui University of Technology, 59 Hudong Road, Maanshan 243002, China
[b] State Key Laboratory of Heavy Oil Processing, China University of Petroleum, Qingdao 266580, China

ARTICLE INFO

Article history:
Received 17 October 2015
Received in revised form
10 January 2016
Accepted 27 February 2016
Available online 2 March 2016

Keywords:
Porous materials
Carbon materials
Interconnected porous carbon
Supercapacitor

ABSTRACT

3D interconnected porous carbons (IPCs) as supercapacitor electrode materials were prepared from MOF-5 via microwave-assisted KOH activation. The results show that the BET surface area of as-made IPCs is tunable from 798 to 1595 $m^2 g^{-1}$. $IPC_{3\text{-}M}$ made at 3 of MOF-5/KOH mass ratio shows a high capacitance up to 212 $F g^{-1}$ in 6 m KOH aqueous electrolyte at a current density of 0.05 $A g^{-1}$. IPC electrodes also exhibit excellent rate capability (82.9% capacitance retention as the current density increases from 0.05 to 20 $A g^{-1}$) and superior cycle stability (95.9% capacitance retention after 1000 cycles) due to short distance for ion fast transport, abundant accessible pores for ion storage and interconnected architecture for electron conduction.

1. Introduction

Supercapacitors have been used as backup power system for portable electronics or energy storage device for electrical vehicles because of their high power density and long life [1,2]. The electrochemical performance of supercapacitors largely depends on the electrode materials [3]. Porous carbons with high surface area are the most commonly used ones. However, conventional porous carbon-based supercapacitors suffer from low capacitance and poor rate performance due to diffusion limitation related to inner-pore ion transport at high-rate. Thus, synthesis of porous carbons (PCs) with short distance for ion fast transport and abundant accessible pores for ion storage to deliver superior supercapacitive performance remains a big challenge.

Currently, metal organic frameworks (MOFs) or porous coordination polymers have attracted more and more attention, because they can be used as promising templates or carbon precursors to prepare PCs with high surface area [4]. Liu et al. reported that nanoporous carbons, made by polymerizing and carbonizing furfuryl alcohol accommodated in a porous MOF, showed a specific capacitance of 188 $F g^{-1}$ at 0.5 $A g^{-1}$ [5]. Potassium hydroxide (KOH) could be used as the activation agent to synthesize porous materials [6]. The microwave-assisted heating has many advantages over the conventional heating, such as high heating rate and saving of energy [7]. Herein, we report the synthesis of 3D interconnected porous carbons (IPCs) using MOF-5 as carbon precursor and template coupled with microwave-assisted KOH activation.

2. Experimental

First, the MOF-5 was prepared from terephthalic acid and zinc nitrate at room temperature, the details can be found in [8]. Then, the as-made MOF-5 and KOH (analytical grade) were pulverized and mixed in powder state at different mass ratios. The resultant mixture was transferred to a crucible, then put in a quartz protective reactor and heated in a LWMC-205-type microwave oven at the microwave power of 600 W at 20 min heating time in a nitrogen flow (99.999%, 60 ml min^{-1}). After reaction, samples were washed with 2 m hydrochloric (HCl) solution and distilled water for several times to remove the residual ions. Then, IPCs were dried at 383 K for 12 h. The resultant samples are nominated as $IPC_{x\text{-}M}$, of which the subscripts of x and M stand for the mass ratio of MOF-5/KOH and microwave heating, respectively. For comparison, $IPC_{x\text{-}C}$ was also prepared at a heating rate of 5 K min^{-1} to 1123 K in flowing nitrogen by conventional heating, in which the subscript C refers to conventional heating. The morphology and microstructure of obtained IPCs were investigated by transmission electron microscopy (TEM, JEOL-2100), X-ray diffraction (XRD, Philips X, pert Prosuper, CuKα, Radiation), and nitrogen (N_2) adsorption. The electrode of symmetrical supercapacitor was fabricated by mixing IPCs, carbon black and poly (tetrafluoroethy-lene) in a weight ratio of 83:5:12. The electrochemical performance of supercapacitors was evaluated in 6 m KOH aqueous electrolyte,

* Corresponding authors.
E-mail addresses: xjhe@ahut.edu.cn, agdxjhe@126.com (X. He), wumb@upc.edu.cn (M. Wu).

http://dx.doi.org/10.1016/j.matlet.2016.02.144
0167-577X/

further information can be found in [7].

3. Results and discussion

Fig. 1a shows the schematic of the fabrication process of IPCs. The TEM images of samples after acid treatment are shown in Fig. 1b–e. PCs in Fig. 1b–e are almost transparent to electron beams, demonstrating extremely thin thickness, e.g. short distance for ion fast transport. The interconnected parts mean good electron conduction.

Fig. 2a shows the XRD patterns of the IPC samples. It is seen that all IPCs are amorphous because there are only weak and broad (002) peaks at about 26–29°, and (100) peaks at about 40–48°. XRD results in Fig. 2a show that no residual Zn and K elements exist in IPCs. Fig. 2b presents the XRD patterns of $IPC_{4\text{-}M}$ sample in terms of the unwashed IPCs, IPCs only washed by water, and IPCs washed by both water and HCl. In general, potassium carbonate (K_2CO_3, JCPDS no. 16-0820) still exists in unwashed $IPC_{4\text{-}M}$. Some K-containing compounds are produced due to the possible reaction between KOH and carbon according to Eq. (1) [9].

$$6KOH + 2C \rightarrow 2K + 3H_2 + 2K_2CO_3 \quad (1)$$

Nevertheless, K-containing compounds disappear from the IPCs washed by distilled water while the diffraction peak of zinc oxide (ZnO, JCPDS no. 36-1451) is observed. As the decomposition product of MOF-5 at high temperature [10], ZnO can be easily removed from IPCs by using both distilled water and 2 m HCl solution because no diffraction peaks of ZnO exist in this sample, as shown in Fig. 2b.

N_2 adsorption-desorption isotherms and pore size distribution of all the IPC samples are shown in Fig. 2c–d. The pore structure parameters of IPCs are shown in Table 1. Fig. 2c shows that only $IPC_{1\text{-}M}$ is microporous carbon evidenced by the Type I isotherms in accordance with the IUPAC classification with smaller MOF-5/KOH mass ratio of 1, while all the other samples are mesoporous carbons evidenced by the pronounced hysteresis loop in the N_2 adsorption-desorption isotherms. With the increasing MOF-5/KOH mass ratio (ranging from 1 to 5), the D_{ap}, V_t and Non-V_{mic} of IPCs increase. The S_{BET} of IPC made at 4:1 of MOF-5/KOH mass ratio achieves its peak value of 1595 $m^2 g^{-1}$. It is noted that the S_{BET} and V_t of $IPC_{2\text{-}M}$ are relatively smaller than those of $IPC_{2\text{-}C}$ except the D_{ap} value due to the rapid heating rate of microwave (30 K min^{-1} for $IPC_{2\text{-}M}$ while only 5 K min^{-1} for $MNC_{2\text{-}C}$). Fig. 2d shows that the micropores of IPCs mainly center at 0.4–0.9 nm and 1.1–1.8 nm, and the mesopores of IPCs center at 2–5 nm. The inset in Fig. 2d shows that some mesopores of $IPC_{5\text{-}M}$ center at 8–9 nm and 12–15 nm while that of $IPC_{4\text{-}M}$ and $IPC_{3\text{-}M}$ center at 18–48 nm.

Fig. 3a shows the CV curves of $IPC_{3\text{-}M}$ at different scan rates in

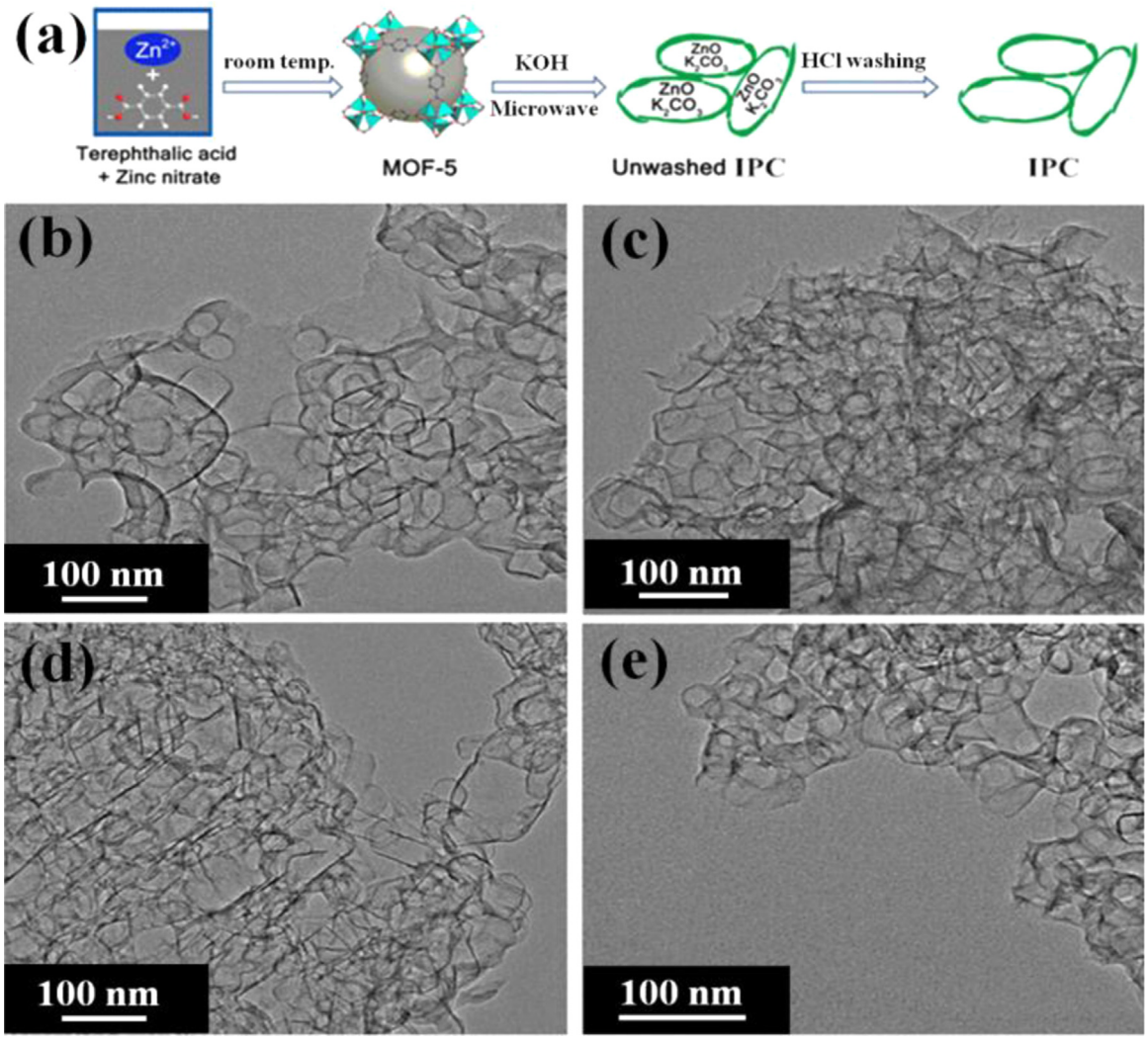

Fig. 1. (a) Fabrication schematic of 3D IPCs. TEM images of (b) $IPC_{2\text{-}M}$, (c) $IPC_{3\text{-}M}$, (d) $IPC_{4\text{-}M}$, (e) $IPC_{5\text{-}M}$.

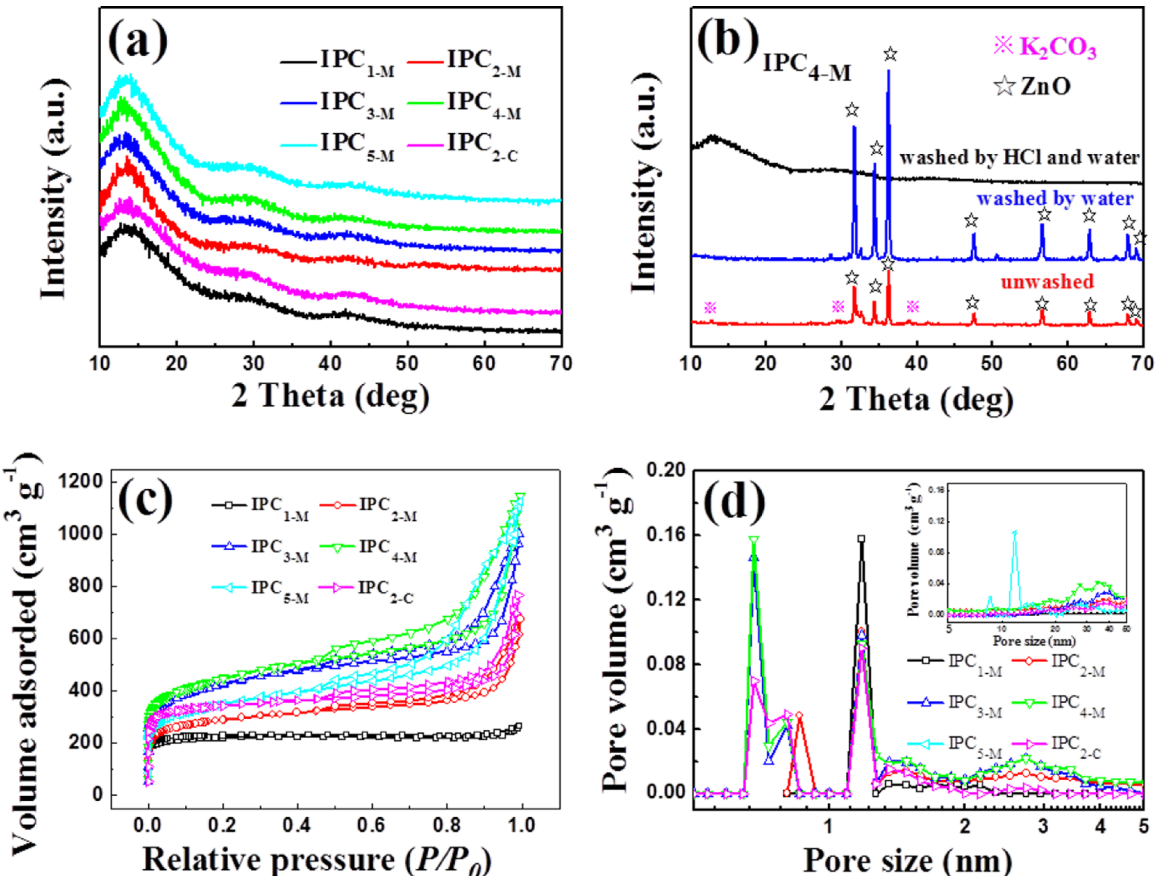

Fig. 2. (a) XRD patterns of IPCs; (b) XRD patterns of $IPC_{4\text{-}M}$ before and after washing; (c) N_2 adsorption-desorption isotherms; (d) pore size distribution of IPCs.

Table 1
Pore structure parameters of IPCs in different masses.

Samples	D_{ap} (nm)	S_{BET} ($m^2\ g^{-1}$)	S_{mic} ($m^2\ g^{-1}$)	V_t ($cm^3\ g^{-1}$)	V_{mic} ($cm^3\ g^{-1}$)	Non-V_{mic} ($cm^3\ g^{-1}$)	Mass (g)
$IPC_{1\text{-}M}$	1.94	798	800	0.39	0.35	0.04	0.79
$IPC_{2\text{-}M}$	3.05	1041	869	0.79	0.40	0.39	1.22
$IPC_{3\text{-}M}$	3.39	1515	1245	1.28	0.60	0.68	1.19
$IPC_{4\text{-}M}$	3.76	1595	1265	1.50	0.60	0.90	0.95
$IPC_{5\text{-}M}$	4.88	1247	896	1.52	0.43	1.09	0.77
$IPC_{2\text{-}C}$	2.82	1219	1070	0.86	0.48	0.38	1.19

6 m KOH aqueous electrolyte. It can be found that the CV curves of $IPC_{3\text{-}M}$ electrode almost retain the symmetric rectangular shape with the increasing scan rate from 2 to 200 mV s^{-1}. Fig. 3b shows the CV curves of IPC electrodes at 200 mV s^{-1} scan rate. The rectangular CV curves of IPCs even at a high scan rate of 200 mV s^{-1} reflect the rapid ion diffusion in IPCs. The area of CV curves reflects the capacitance value, in which $IPC_{3\text{-}M}$ electrode shows the biggest capacitance. Fig. 3c shows the specific capacitance of IPC electrodes at different discharge current densities. The specific capacitance of $IPC_{3\text{-}M}$ electrode is the biggest among all the IPC electrodes, reaching 212 F g^{-1} at 0.05 A g^{-1} and 175 F g^{-1} at 20 A g^{-1}, with the capacitance retention of 82.5%, which are consistent with its bigger S_{BET} and D_{ap}. It is reported that the capacitance of MC-Zn made by direct carbonization of MOF-5 is 95 F g^{-1} at 0.5 A g^{-1} [11]. Note that the reported nanoporous carbon made by polymerizing and then carbonizing carbon precursor at 800 °C (NPC_{800}) shows 151 F g^{-1} of specific capacitance at 0.05 A g^{-1}, displaying the capacitance retention of 74% when the current density was increased to 0.5 A g^{-1} [5]. As for $IPC_{3\text{-}M}$ electrode, its specific capacitance remains at 199 F g^{-1} at 0.8 A g^{-1}. Obviously, the capacitance performance of $IPC_{3\text{-}M}$ is superior to those of MC-Zn and NPC_{800} reported in literature. With the increase of discharge current density from 0.05 to 20 A g^{-1}, the capacitance retention of all the IPC electrodes is in the range of 76.9%–85.6%, showing perfect rate performance. Fig. 3d is the variation of specific capacitance retention of $IPC_{3\text{-}M}$ electrodes versus cycle number in two electrode system. The capacitance retention of $IPC_{3\text{-}M}$ remains at 95.9% after 1000 charge-discharge cycles, showing excellent cycle stability. The inset in Fig. 3d shows the electrochemical impedance spectroscopy (EIS) of $IPC_{3\text{-}M}$ electrodes. The low *x*-intercept (0.49 Ω), small diameter of the semicircle and high slope at low frequency reveal that the $IPC_{3\text{-}M}$ electrode has low internal resistance and charge-discharge resistance, and excellent pore accessibility.

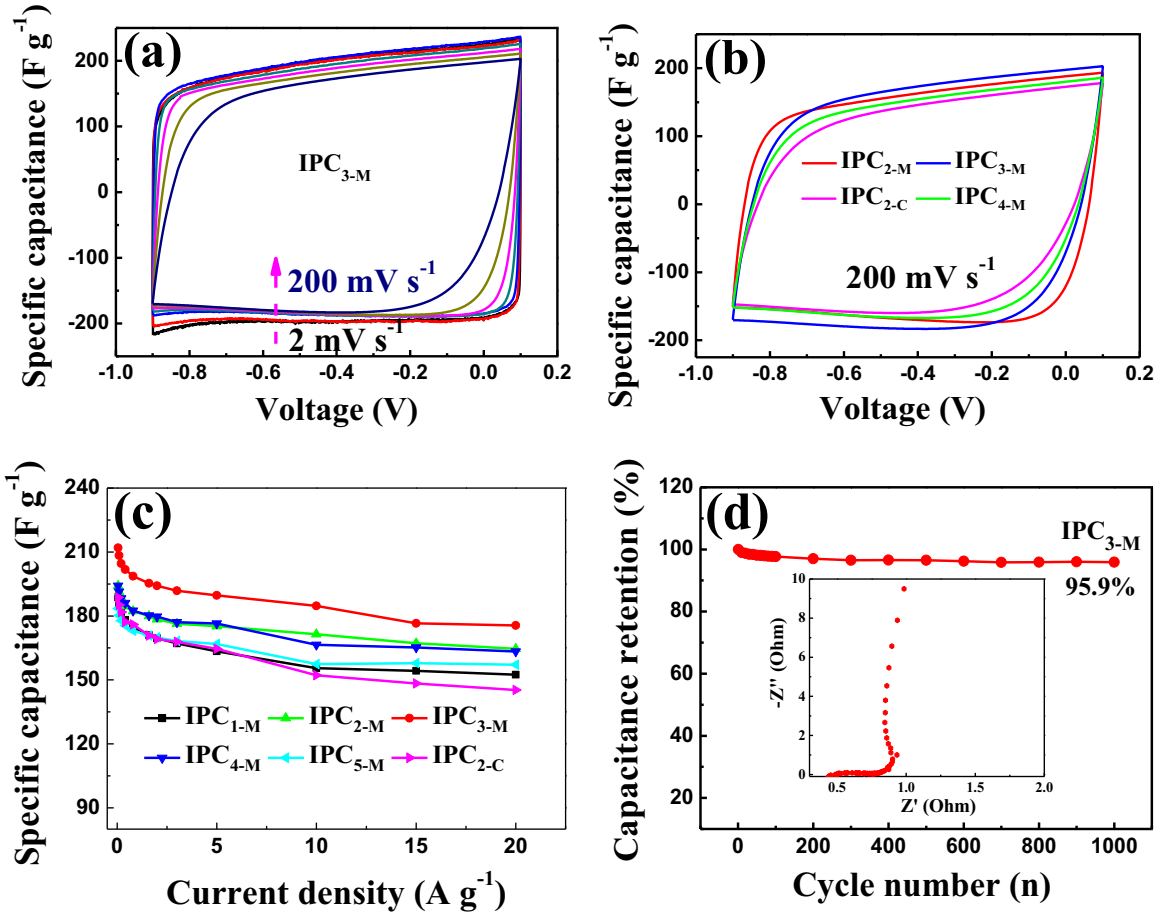

Fig. 3. (a) CV curves of $IPC_{3\text{-}M}$ electrode at different scan rates in 6 m KOH aqueous electrolyte (b) CV curves of IPC electrodes at 200 mV s^{-1}; (c) Specific capacitance of IPC electrodes vs. current density; (d) Specific capacitance of $IPC_{3\text{-}M}$ electrode vs. cycle number.

4. Conclusions

3D IPCs for supercapacitors have been prepared from MOF-5 by a microwave-assisted KOH activation. The results show that these IPCs feature short distance for ion fast transport, abundant accessible pores for ion storage and interconnected architecture for good electron conduction. The advanced overall performance has been optimized for $IPC_{3\text{-}M}$, which shows high capacitance (212 F g^{-1} in 6 m KOH at 0.05 A g^{-1}), good rate capability and superior cycle stability (95.9% capacitance retention after 1000 cycles). The findings highlight a novel method to synthesize 3D interconnected materials for energy storage.

Acknowledgements

This work was partly supported by the NSFC (Nos. 51272004 and U1361110), the Program for New Century Excellent Talents in University of the Education Ministry of China (No. NCET-13-0643).

References

[1] H.X. Luo, Z.Y. Liu, L.M. Chao, X.C. Wu, X.D. Lei, Z. Chang, et al., J. Mater. Chem. A 3 (2015) 3667–3675.
[2] Y. Gao, L. Li, Y.M. Jin, Y. Wang, C.J. Yuan, Y.J. Wei, et al., Appl. Energy 153 (2015) 41–47.
[3] X.J. He, H.B. Zhang, H. Zhang, X.J. Li, N. Xiao, J.S. Qiu, J. Mater. Chem. A 2 (2014) 19633–19640.
[4] Y.M. Liu, X. Quan, X.F. Fan, H. Wang, S. Chen, Angew. Chem. Int. Ed. 54 (2015) 6837–6841.
[5] B. Liu, H. Shioyama, H.L. Jiang, X.B. Zhang, Q. Xu, Carbon 48 (2010) 456–463.
[6] H.L. Wang, Q.M. Gao, J. Hu, J. Am. Chem. Soc. 131 (2009) 7016–7022.
[7] X.J. He, R.C. Li, J.S. Qiu, K. Xie, P.H. Ling, M.X. Yu, et al., Carbon 50 (2012) 4911–4921.
[8] L.M. Huang, H.T. Wang, J.X. Chen, Z.B. Wang, J.Y. Sun, D.Y. Zhao, et al., Microporous Mesoporous Mater. 58 (2003) 105–114.
[9] J.C. Wang, S. Kaskel, J. Mater. Chem. 22 (2012) 23710–23725.
[10] B. Liu, H. Shioyama, T. Akita, Q. Xu, J. Am. Chem. Soc. 130 (2008) 5390–5391.
[11] X.L. Yan, X.J. Li, Z.F. Yan, S. Komarneni, Appl. Surf. Sci. 308 (2014) 306–310.